

- dam (1982).
6. J. H. Newton, R. A. Levine and W. B. Person, *J. Chem. Phys.* **67**, 3282 (1977).
 7. B. Galabov, T. Dudev and W. J. Orville-Thomas, *J. Mol. Struct.* **145**, 1 (1986).
 8. K. Kim and C. W. Park, *J. Mol. Struct.* **161**, 297 (1987).
 9. W. T. King and G. B. Mast, *J. Phys. Chem.* **80**, 2521 (1976).
 10. W. B. Person, B. Zilles, J. D. Rogers and R. G. A. Maia, *J. Mol. Struct.* **80**, 297 (1982).
 11. K. Kim, *J. Phys. Chem.* **88**, 2394 (1984).
 12. E. B. Wilson, Jr., J. C. Decius and P. C. Cross, *Molecular vibrations*, McGraw-Hill, New York (1955).
 13. K. Kim, R. S. McDowell and W. T. King, *J. Chem. Phys.* **73**, 36 (1980).
 14. C. A. Coulson, *Spectrochim. Acta* **14**, 161 (1959).
 15. J. C. Decius, *J. Mol. Spectrosc.* **57**, 348 (1975).
 16. J. S. Binkley, M. J. Frisch, D. J. DeFrees, K. Raghavachari, R. A. Whiteside, H. B. Schlegel, G. Flueter and J. A. Pople, Carnegie-Mellon Chemistry Publication Unit, Pittsburgh, PA (1983).
 17. J. L. Duncan, D. C. McKean and G. K. Speirs, *Mol. Phys.* **24**, 553 (1972).
 18. J. L. Duncan, D. A. Lawie, G. D. Nivellini, F. Tullini, A. M. Ferguson, J. Harper and K. H. Tonge, *J. Mol. Spectrosc.* **121**, 294 (1987).
 19. A. Ruoff and H. Burger, *Spectrochim. Acta* **26A**, 989 (1970).
 20. M. Jen and D. R. Lide, *J. Chem. Phys.* **36**, 2525 (1962).
 21. E. R. Cohen and B. N. Taylor, *J. Phys. Chem. Ref. Data* **2**, 663 (1973).
 22. J. H. Newton and W. B. Person, *J. Chem. Phys.* **64**, 3036 (1976).
 23. K. Kim and W. T. King, *J. Chem. Phys.* **80**, 978 (1984).
 24. W. T. King, G. B. Mast and P. P. Blanchette, *J. Chem. Phys.* **56**, 4440 (1972); **58**, 1272 (1973).
 25. K. Kim and W. T. King, *J. Chem. Phys.* **80**, 983 (1984).
 26. K. Kim and H. G. Lee, *Bull. Kor. Chem. Soc.* **6**, 79 (1985).
 27. H. B. Schlegel, S. Wolfe and F. Bernardi, *J. Chem. Phys.* **67**, 4194 (1977).
 28. K. Tanabe and S. Saeki, *Spectrochim. Acta* **26A**, 1469 (1970).
 29. R. W. Davis, A. G. Robiette and M. C. L. Gerry, *J. Mol. Spectrosc.* **85**, 399 (1981).
 30. J. W. Russell, C. D. Needham and J. Overend, *J. Chem. Phys.* **45**, 3383 (1966).
 31. S. Saeki and K. Tanabe, *Spectrochim. Acta* **25A**, 1325 (1969).

Kinetic Energy Release in the Fragmentation of *tert*-Butylbenzene Molecular Ions. A Mass-analyzed Ion Kinetic Energy Spectrometric(MIKES) Study

Joong Chul Choe, Byung Joo Kim, and Myung Soo Kim*

Department of Chemistry, College of Natural Sciences,
Seoul National University, Seoul 151-742. Received December 6, 1988

Kinetic energy release in the fragmentation of *tert*-butylbenzene molecular ion was investigated using mass-analyzed ion kinetic energy spectrometry. Method to estimate kinetic energy release distribution (KERD) from experimental peak shape has been explained. Experimental KERD was in good agreement with the calculated result using phase space theory. Effect of dynamical constraint was found to be important.

Introduction

Studies of the ion structure and the fragmentation mechanism are of primary concern for the fundamental understanding of mass spectrometry.¹⁻¹³ Especially, the role of ion internal energy and its disposal in the fragmentation are subjects of profound interest in physical chemistry.¹⁻³ From these perspectives, various mass spectrometric methods have been developed such as metastable ion mass spectrometry,^{4,5} collisional activation mass spectrometry,^{6,7} field ionization kinetics,⁸ photodissociation mass spectrometry,^{9,10} and photoelectron-photoion coincidence spectrometry.¹¹ Also, some of these techniques find increasing use in analytical application.^{12,13}

Theoretically, ion fragmentation kinetics is usually des-

cribed by the quasi-equilibrium theory(QET) proposed by Rosenstock *et al.*,¹⁴ Since quasi-equilibrium assumption in QET leads to the same mathematical formalism as the Rice-Ramsperger-Kassel-Marcus (RRKM) theory¹⁵ for unimolecular reaction, this is sometimes called the RRKM-QET theory. A unimolecular reaction can also be investigated from the corresponding reverse reaction relying on the principle of microscopic reversibility. The phase space theory (PST) developed by Light *et al.*¹⁶⁻²⁰ and by Klotz²¹⁻²⁴ from this prospective has proved useful for the understanding of ion fragmentation process. Especially, PST has provided a good description of the disposal of the internal energy of a fragmenting ion to the kinetic energy of the products.²⁴⁻³¹

In the present work, a metastable ion decomposition has been investigated for the molecular ion of *tert*-butylbenzene.

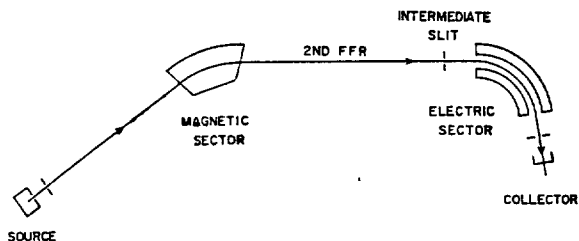
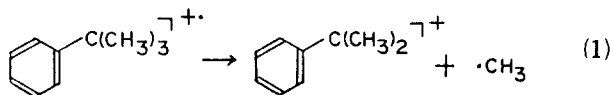


Figure 1. Ion-optical configuration of VG ZAB-E reversed geometry double focusing mass spectrometer.



Kinetic energy release in the fragmentation reaction has been estimated from the metastable peak shape and compared with the PST calculation.

Experimental

The instrument used in this work was VG Analytical model ZAB-E double focusing mass spectrometer with reversed geometry. The schematic diagram for the ion-optical system of this instrument is shown in Figure 1. Ions formed in the source are accelerated and mass-selected by the magnetic sector. For the metastable ion decomposition occurring in the second field-free region (2nd FFR), namely between the magnetic sector and the electric sector,



the translational energy of the daughter ion (m_2^+) is approximately given by

$$E_2 = (m_2/m_1)eV \quad (3)$$

Here, eV is the translational energy of the parent (m_1^+). In the mass-selected ion kinetic energy spectrometry (MIKES) used in this work, the daughter ions are analyzed by scanning the potential applied to the electric sector which is a translational energy analyzer.

tert-Butylbenzene (TBB) was introduced to the ion source using the septum inlet and ionized by 70 eV electron ionization. Trap current was 200 μA , the source temperature was 200 $^\circ\text{C}$ and 8 kV accelerating voltage was used. The width of the intermediate slit was set such that the effect of instrumental line broadening on the metastable peak shape was negligible. Because the signal intensity was rather weak (3×10^{-13} Amp), signal averaging was performed for 40 repetitive scans using a data system. The best grade of *tert*-butylbenzene commercially available was used without further purification. Its purity was checked by mass spectrometry.

Peak Shape Analysis

As an ion fragments, some of its internal energy is released as the kinetic energy of the product ion and the neutral in the center-of-mass coordinate system. The product ion velocity in the laboratory coordinate is the vector sum of its velocity in the center-of-mass coordinate and the velocity of center-of-mass coordinate itself. Hence, the product ion translational energy will show a certain distribution depending on

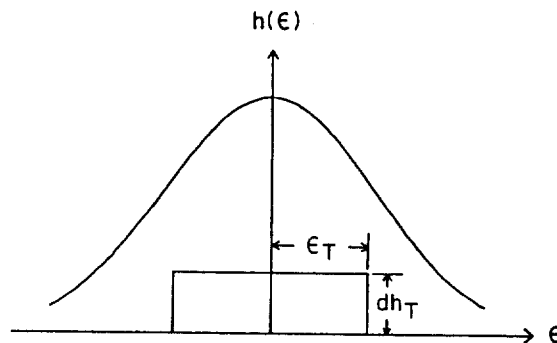


Figure 2. A schematic metastable peak shape. The rectangle is a contribution from kinetic energy release in the range T to $T + dT$. See text for symbols.

the direction of fragmentation with respect to the ion-optical trajectory even when a unique amount of kinetic energy is released. Such a translational energy distribution results in broad linewidth of a metastable peak. According to Beynon and coworkers,^{32,33} the metastable peak due to the reaction (2) with a unique kinetic energy release (T) occurring at the intermediate focal point of a reversed geometry instrument has a rectangular shape with a half width (ϵ_T) given by

$$\frac{\epsilon_T}{eV} = \frac{2m_2}{m_1} \left(\frac{m_2 T}{m_2 eV} \right)^{1/2} \quad (4)$$

This equation can be rearranged as follows

$$T = \gamma \epsilon_T^2 \quad (5)$$

with

$$\gamma = \frac{m_1^2}{4m_2 m_3 eV} \quad (6)$$

In most of the metastable ion decomposition reactions, however, the kinetic energy releases are not unique values, but have certain distributions. Hence, the resulting metastable peaks tend to have smooth and rather monotonic shapes. Various methods have been proposed to calculate kinetic energy release distribution (KERD) from a metastable peak shape. Holmes and Osborne³⁴ used an analytical trial function for KERD to fit a metastable peak. Beynon and coworkers³⁵ developed a graphical method to derive KERD from the peak shape. More recently, Jarrold *et al.*³⁶ showed that KERD can be obtained by taking the first derivative of the peak shape function. Here, a more general and detailed formalism will be presented which provides the same result as the above ones in simple cases.

With the kinetic energy release distribution $n(T)$, the probability to release the kinetic energy in the range T to $T + dT$ is given by $n(T)dT$. The metastable peak rectangle produced by such a reaction will have the width $2\epsilon_T$ and the height of dh_T satisfying the following relation.

$$n(T) dT = 2\epsilon_T dh_T \quad (7)$$

With the coordinate transformation $E - E_2 \rightarrow \epsilon$ where E is the translational energy axis (x -axis) for the metastable peak shape, this rectangle can be drawn as in Figure 2. From the figure it is clear that only those product ions with KER satisfying the following condition contribute to the peak height at ϵ

$$T \geq \gamma \epsilon^2 \quad (8)$$

agreement with the experimental results because the degrees of freedom of the transition state moiety do not directly correspond to product vibrations, rotations, and translations.⁴⁰ In the phase space theory version of RRKM-QET formulated by Klotz,²¹⁻²⁴ it was postulated that the long-range charge-induced dipole interaction dominated the potential. Then, PST is equivalent to RRKM-QET for "loose" transition state. Recently, Chesnavich and Bowers^{25,26} have further advanced the theory by developing rigorous classical method for determining phase space volumes. Since the "loose" transition state is near the product region and angular momentum is conserved, the theory is very useful for predicting product state distributions, especially, KERD.

In phase space theory, KERD is evaluated subject to constraints arising from conservation of energy, conservation of angular momentum, and the effect of the centrifugal barrier to reaction. Energy conservation is given by

$$E = T + V + R \quad (13)$$

where E is the total available energy or excess energy for fragments and T , V , and R are translational, vibrational, and rotational energy of fragments, respectively. Angular momentum conservation is given by

$$\vec{J} = \vec{L} + \vec{J}' \quad (14)$$

where \vec{J} is the angular momentum of parent, \vec{L} is the orbital angular momentum of products, and \vec{J}' is the vector sum of the rotational angular momenta of products. The available phase space is determined by the above constraints and the effect of the centrifugal barrier. As the orbital angular momentum gets larger, the centrifugal barrier increases accordingly.²⁵ Hence, for a given translational energy the orbital angular momentum should be less than a certain maximum value for the reaction to occur. Namely, the dynamical constraint will reduce the size of the available phase space volume.

Then, the probability for a parent with energy E and angular momentum J to release kinetic energy T , namely KERD is given by

$$n(T, J, E) = A \int_{R^*}^{E-T} \rho(E-T-R) P(T, J, R) dR \quad (15)$$

Here, ρ and P are vibrational and angular momentum state densities for the products, respectively, and R^* is the minimum rotational energy of the products that can satisfy the constraints. A is the normalization constant to satisfy the following condition.

$$\int n(T, J, E) dT = 1 \quad (16)$$

Chesnavich and Bowers^{25,28} have derived analytical expressions of $P(T, J, R)$ for several product symmetries. Their results have been utilized to calculate KERD in the present work. More recently, Chesnavich and coworkers²⁹⁻³¹ have proposed a method to evaluate $P(T, J, R)$ by quantum mechanical state counting. A calculation with the computer program by these workers resulted in virtually the same KERD as above.

Since the rotational angular momenta of molecular ions produced in the ion source exhibit Boltzman distribution, $n(T, J, E)$ obtained above should be averaged over J to compare with the experimental result.

Table 1. Molecular Parameters used in the Phase Space Theoretical Calculation

I. Vibrational frequencies, ^a cm ⁻¹		ϵ	
C ₉ H ₁₁ ⁺ ^b			·CH ₃ ^f
3060(2)	1280	770	3100(2)
3030(2)	1220	740	3000
3000	1190	690	1400(2)
2950(4)	1160	620	800
2900	1150(2)	600	
2890	1080	530	
1610	1030	440	
1580	1000	390	
1510	990	380	
1460	960	300	
1450(4)	920(2)	270	
1400(2)	870	200(2)	
1370(2)	840	150	
1310	800		
II. Rotational constant, ^d cm ⁻¹			
C ₁₀ H ₁₄ ⁺ ^b	0.0449		
C ₉ H ₁₁ ⁺ ^b	0.0507		
·CH ₃ ^c	7.644		
III. Polarizability, Å ³			
·CH ₃ ^c	2.20		

^aNumbers in the parentheses denote the degeneracies of vibrational modes. ^bEstimated values. See text. ^cReference 25. ^dAll species were treated as spherical top molecules. See text for details.

$$n(T, E) = \frac{\sum_j g_j \exp(-R_0/kT_0) n(T, J, E)}{\sum_j g_j \exp(-R_0/kT_0)} \quad (17)$$

Here R_0 is the parent rotational energy, g_j is the rotational degeneracy, and T_0 is the source temperature. In the present work, $n(T, J, E)$ was evaluated with the root-mean-square J value. KERD thus calculated was the same as the rotationally averaged result within experimental error.

To evaluate KERD, various structural parameters for parent and products are needed. The product ion was assumed to have dimethylbenzyl structure.^{8,11} Its vibrational frequencies were estimated referring to those of α -methylstyrene, cumene, and N,N-dimethylaniline.⁴¹ Rotational constants of *tert*-butylbenzene and dimethylbenzyl cations were estimated from their structures. Data for methyl radical were taken from Reference 25. In the calculation of rotational state density, the products were approximated as spherical tops with the rotational constants equal to geometrical mean of their rotational constants ($(ABC)^{1/3}$). Discrepancy due to this approximation was reported as negligible.²⁸ Structural parameters used in the calculation are listed in Table 1.

To calculate KERD, the internal energy(E) or its distribution of the parent ion above the zero point of the potential energy surface of the products is needed. Unfortunately, such information is not available for ions generated by electron ionization. However, it is well known that the internal energy contents of the ions contributing to metastable peaks have very narrow distribution due to a kinetic reason.^{1,2} One way to estimate the internal energy distribution of metastable ions is to use the rate constants calculated by RRKM-

QET. This approach, however, may introduce further ambiguities on the calculated KERD. In the present work, the internal energy was treated as an independent parameter. This was varied such that a good fit between the experimental and calculated KERD's could be achieved. A good fit was determined using statistical least squares method. The best agreement between the experimental and calculated KERD's was achieved when the parent ion internal energy referred to the products ground level was 0.19 eV. The calculated result is shown in Figure 4. When the internal energy differed from the above value by ± 0.02 eV or more, the calculated KERD deviated noticeably from the experimental one, especially at small T . In particular, when the internal energy value of 0.25 eV was used to minimize the discrepancy between the experimental and the calculated KERD's at high T , the probability at the curve maximum decreased by around 20%. The apparent discrepancy at high T region of Figure 4, if meaningful, may be attributed to the contribution from the metastable decomposition of the parent ions with internal energy larger than the average value. However, the fact that experimental KERD can be explained extremely well by PST calculation supports the validity of the average value approach adopted here. More importantly, this indicates that the fragmentation proceeds statistically.

Recently, Brand and Baer¹¹ investigated the kinetics and energetics of the same process using photoelectron-photoion coincidence technique (PEPICO). The ionization energy (IE) of TBB thus obtained was 8.63 ± 0.01 eV and the appearance energy (AE) of dimethylbenzyl cation from TBB was 9.93 ± 0.03 eV. Using the critical energy of 1.30 ± 0.04 eV for the dissociation process estimated by (AE-IE), a good fit between the experimental and calculated (RRKM) rate constants was reported. Neglecting the reverse activation energy, 0.19 eV of parent internal energy referred to the product states found in the present work corresponds to 1.49 ± 0.04 eV when referred to the parent zero-point energy. Then, comparing with the experimental rate constant *vs* internal energy relationship reported by Brand and Baer, parent ions with internal energy in this range will dissociate with rate constant 1×10^4 – 2×10^4 sec⁻¹. In the present experiment, the rate constant for the process occurring in the second field-free region can be estimated roughly from ion flight time. Assuming $2.8 \pm 2 \mu$ sec ion residence time in the source,⁴² the parent ions would stay in the second field-free region between 18 and 31μ sec after formation. Then, the average rate constant for the process detected by the present method will be in the range 2×10^4 – 3×10^4 sec⁻¹. This is in good agreement with the results reported by Brand and Baer.

The same process was investigated also by Brand and Levsen⁸ using field ionization kinetic (FIK) method. Experimental rate constant was measured as a function of parent ion internal energy. Even though rate constant *vs* internal energy relationship showed substantial uncertainties originating from experimental difficulties, the experimental results were reported to be in good overall agreement with the calculated (RRKM) results. Since Brand and Levsen used 1.14 ± 0.02 eV as the critical energy of the process, average internal energy estimated for present work corresponds to 1.33 ± 0.02 eV referred to the zero-point energy of the parent. The experimental rate constants measured by Brand and Levsen for the parent ion with this internal energy ran-

ges from $\sim 10^3$ sec⁻¹ to 6×10^4 sec⁻¹ which is again in good agreement with the present estimation. In summary, both the rate constant and KERD found in this work indicate that the dissociation process (1) occurs statistically.

The statistically expected average kinetic energy release is frequently evaluated by^{11,22-24}

$$\bar{E} = \bar{T} + \bar{R} + \bar{V} \\ = kT^* + \frac{r-1}{2} kT^* + \sum_i \frac{h\nu_i}{\exp(h\nu_i/kT^*) - 1} \quad (18)$$

Here, r , ν_i , and T^* are rotational degree of freedom, vibrational frequencies, and effective temperature of the products, respectively. The average kinetic energy release (\bar{E}) evaluated by this formula is 23 meV which is smaller than the experimental value of 30 meV. To account for this discrepancy, details of phase volume calculation were looked into. It was found that such a discrepancy originated from the dynamical constraint for overcoming the centrifugal barrier. In the present system, since the reduced rotational constant and the reduced mass of the products were abnormally small, the maximum orbital angular momentum had to be small. Hence, many parts of the phase space accessible under the energy and momentum constraints were not available under the dynamical constraint, resulting in the increase of kinetic energy release.

In summary, it can be concluded that the process (1) occurs statistically and that the effect of the dynamical constraint plays an important role in the process.

Acknowledgement. Authors wish to thank Prof. T. Matsuo for providing TRIO program and Prof. W. J. Chesnavich for providing PST program (state counting). This work was supported financially by Yukong Ltd..

References

1. M. S. Kim, "Mass Spectrometry", Mineumsa, Seoul, 1987.
2. K. Levsen, "Fundamental Aspects of Organic Mass Spectrometry", Verlag Chemie, Weinheim, 1978.
3. R. G. Cooks, J. H. Beynon, R. M. Caprioli, and G. R. Lester, "Metastable Ions", Elsevier, Amsterdam, 1973.
4. M. A. Hanratty, J. L. Beauchamp, A. J. Illies, P. van Koppen, and M. T. Bowers, *J. Am. Chem. Soc.* **110**, 1 (1988).
5. Y. Malinovich, R. Arakawa, G. Haase, and C. Lifshitz, *J. Phys. Chem.* **89**, 2253 (1985).
6. M. S. Kim and F. W. McLafferty, *J. Am. Chem. Soc.* **78**, 3279 (1978).
7. M. Rabrenović, J. H. Beynon, S. H. Lee, and M. S. Kim, *Int. J. Mass Spectrom. Ion. Processes* **65**, 197 (1985).
8. W. A. Brand and K. Levsen, *Int. J. Mass Spectrom. Ion Phys.* **51**, 135 (1983).
9. M. S. Kim, R. C. Dunbar, and F. W. McLafferty, *J. Am. Chem. Soc.* **100**, 4600 (1978).
10. H. S. Kim, M. F. Jarrold, and M. T. Bowers, *J. Chem. Phys.* **84**, 4882 (1986).
11. W. A. Brand and T. Baer, *Int. J. Mass Spectrom. Ion Phys.* **49**, 103 (1983).
12. Y. J. Kim, J. C. Choe, and M. S. Kim, *Bull. Korean Chem. Soc.*, **10**, 15 (1989).
13. F. W. McLafferty, Ed., "Tandem Mass Spectrometry",

- Wiley, New York, 1983.
14. H. M. Rosenstock, M. B. Wallenstein, A. L. Wahrhaftig, and H. Eyring, *Pro. Nat. Acad. Sci. U.S.* **38**, 667 (1952).
 15. P. J. Robinson and K. A. Holbrook, "Unimolecular Reactions", Wiley, New York, 1972.
 16. J. C. Light, *J. Chem. Phys.* **40**, 3221 (1964).
 17. P. Pechukas and J. C. Light, *J. Chem. Phys.* **42**, 3281 (1965).
 18. J. C. Light and J. Lin, *J. Chem. Phys.* **43**, 3209 (1965).
 19. J. C. Light, *Discuss. Faraday Soc.* **44**, 14 (1967).
 20. E. Nikitin, *Theor. Exp. Chem. (USSR)* **1**, 144 (1965).
 21. C. E. Klots, *J. Phys. Chem.* **75**, 1526 (1971).
 22. C. E. Klots, *Z. Naturforsch.* **27A**, 553 (1972).
 23. C. E. Klots, *J. Chem. Phys.* **58**, 5364 (1973).
 24. C. E. Klots, *J. Chem. Phys.* **64**, 4269 (1976).
 25. W. J. Chesnavich and M. T. Bowers, *J. Am. Chem. Soc.* **98**, 8301 (1976).
 26. W. J. Chesnavich and M. T. Bowers, *J. Am. Chem. Soc.* **99**, 1705 (1977).
 27. K. Johnson, I. Powis, and C. J. Danby, *Chem. Phys.* **63**, 1 (1981).
 28. W. J. Chesnavich, *Ph. D. Thesis*, University of California, Santa Barbara, California, 1976.
 29. W. J. Chesnavich and M. T. Bowers, *Prog. React. Kinet.* **11**, 137 (1982).
 30. D. A. Webb and W. J. Chesnavich, *J. Phys. Chem.* **87**, 3791 (1983).
 31. W. J. Chesnavich, L. Bass, M. E. Grice, K. Song, and D. A. Webb, *QCPE Bull.* **8**, 557 (1988).
 32. J. H. Beynon, A. E. Fontaine, and G. R. Lester, *Int. J. Mass Spectrom. Ion Phys.* **8**, 341 (1972).
 33. J. E. Szulejko, A. Mendez Amaya, R. P. Morgan, A. G. Brenton, and J. H. Beynon, *Proc. R. Soc. London* **A373**, 1 (1980).
 34. J. L. Holmes and A. D. Osborne, *Int. J. Mass Spectrom. Ion Phys.* **23**, 189 (1977).
 35. A. Mendez Amya, A. G. Brenton, J. E. Szulejko, and J. H. Beynon, *Proc. R. Soc. London* **A373**, 13 (1980).
 36. M. F. Jarrold, W. Wagner-Redeker, A. J. Illies, N. J. Kirchner, and M. T. Bowers, *Int. J. Mass Spectrom. Ion Processes* **58**, 63 (1984).
 37. B. A. Rumpf and P. J. Derrick, *Int. J. Mass Spectrom. Ion Processes* **82**, 239 (1988).
 38. M. S. Kim, Unpublished result.
 39. A. Savitzky and M. J. E. Golay, *Anal. Chem.* **36**, 1627 (1964).
 40. R. A. Marcus, *Discuss. Faraday Soc.* **55**, 381 (1973).
 41. G. Varsanyi, "Assignments for Vibrational Spectra of Seven Hundred Benzene Derivatives", Vol. 1, Halsted Press, New York, 1974.
 42. P. C. Burgers and J. L. Holmes, *Int. J. Mass Spectrom. Ion Processes* **58**, 15 (1984).

Stereoselective Solvolyses of Activated Esters in the Aggregate System of Imidazole-Containing Copolymeric Surfactants

Iwhan Cho*

Department of Chemistry, Korea Advanced Institute of Science and Technology, Seoul 131-650

Burm-Jong Lee

Department of Chemistry, Inje University, Kimhae 621-170. Received December 6, 1988

Stereoselective solvolyses of optically active activated esters in the aggregate system of optically active polymeric surfactants containing imidazole and benzene moieties were performed. The catalyst polymers employed were copolymers of N-methacryloyl-L-histidine methyl ester (MHis) with N,N-dimethyl-N-hexadecyl-N-[10-(p-methacryloyloxyphenoxycarbonyl)-decyl]ammonium bromide (DEMAB). In the solvolyses of N-carbobenzoxy-D- and L-phenylalanine p-nitrophenyl esters (D-NBP and L-NBP) by polymeric catalysts, copoly (MHis-DEMAB) exhibited not only increased catalytic activity but also enhanced enantioselectivity as the mole % of surfactant monomers in the copolymers increased. The polymeric catalysts showed noticeable enantioselective solvolyses toward D- and L-NBP of the substrates employed. As the reaction temperature was lowered for the solvolyses of D- and L-NBP with the catalyst polymer containing 3.5 mole % of MHis, the increased reaction rate and enhanced enantioselectivity were observed. The coaggregate systems of the polymer and monomeric surfactants were also investigated. In the case of coaggregate system consisted of 70 mole % of cetyldimethylethylammonium bromide with polymeric catalyst showed maximum enantioselective catalysis, viz., $k_{\text{cat}}(L)/k_{\text{cat}}(D) = 2.85$. The catalyst polymers in the sonicated solvolytic solutions were confirmed to form large aggregate structure by electron microscopic observation.

Introduction

A great many investigations have been performed regard-

ing the possible alteration of reaction rates in organized media such as micelles, vesicles, polyelectrolytes, and macrocyclic hosts.¹⁻⁷ In most cases, the hydrophobic interac-